Direct field evidence of autocatalytic iodine release from atmospheric aerosol

Tham, Yee Jun

2021-01-26

Tham , Y J , He , X-C , Li , Q , Cuevas , C A , Shen , J , Kalliokoski , J , Yan , C , Iyer , S , Lehmusjärvi , T , Jang , S , Thakur , R C , Beck , L , Kemppainen , D , Olin , M , Sarnela , N , Mikkilä , J , Hakala , J , Marbouti , M , Yao , L , Li , H , Huang , W , Wang , Y , Wimmer , D , Zha , Q , Virkanen , J , Spain , T G , O'Doherty , S , Jokinen , T , Bianchi , F , Petäjä , T , Worsnop , D R , Mauldin , R L , Ovadnevaite , J , Ceburnis , D , Maier , N M , Kulmala , M , O'Dowd , C , Dal Maso , M , Saiz-Lopez , A & Sipilä , M 2021 , ' Direct field evidence of autocatalytic iodine release from atmospheric aerosol ' , Proceedings of the National Academy of Sciences of the United States of America , vol. 118 , no. 4 , 2009951118 . https://doi.org/10.1073/pnas.2

http://hdl.handle.net/10138/328437
https://doi.org/10.1073/pnas.2009951118

Direct field evidence of autocatalytic iodine release from atmospheric aerosol

Yee Jun Tham[a,1], Xu-Cheng He[a], Qinyi Li[b], Carlos A. Cuevas[b], Jiali Shen[a], Joni Kalliokoski[c], Chao Yan[a], Siddharth Iyer[c], Tuuli Lehmusjärvi[a], Sehyun Jang[a,d], Roseline C. Thakur[a], Lisa Beck[a], Deniz Kemppainen[a], Miska Olin[c], Nina Sarnela[a], Jyri Mikkilä[a,e], Jani Hakala[a,e], Marjan Marbouti[a], Lei Yao[a], Haiyan Li[a], Wei Huang[a], Yonghong Wang[a], Daniela Wimmer[a], Qiaozhi Zha[a], Juhani Virkanen[f], T. Gerard Spain[g,h,i], Simon O'Doherty[j], Tuija Jokinen[a], Federico Bianchi[a], Tuukka Petäjä[a], Douglas R. Worsnop[a,k], Roy L. Mauldin III[a], Jurgita Ovadnevaite[g,h,i], Darius Ceburnis[g,h,i], Norbert M. Maier[l], Markku Kulmala[a,m,n], Colin O'Dowd[g,h,i], Miikka Dal Maso[c], Alfonso Saiz-Lopez[b,2], and Mikko Sipilä[a,2]

[a]Institute for Atmospheric and Earth System Research/Physics, Faculty of Science, University of Helsinki, 00014 Helsinki, Finland; [b]Department of Atmospheric Chemistry and Climate, Institute of Physical Chemistry Rocasolano, CSIC, Madrid 28006, Spain; [c]Aerosol Physics Laboratory, Physics Unit, Tampere University, FI-33014 Tampere, Finland; [d]Division of Environmental Science and Engineering, Pohang University of Science and Technology, 37673 Pohang, Korea; [e]Karsa Ltd., 00560 Helsinki, Finland; [f]Department of Geosciences and Geography, University of Helsinki, 00560 Helsinki, Finland; [g]School of Physics, National University of Ireland Galway, H91 CF50 Galway, Ireland; [h]Ryan Institute's Centre for Climate & Air Pollution Studies, National University of Ireland Galway, H91 CF50 Galway, Ireland; [i]Marine Renewable Energy Ireland, National University of Ireland Galway, H91 CF50 Galway, Ireland; [j]School of Chemistry, University of Bristol, BS8 1TS Bristol, United Kingdom; [k]Aerodyne Research Inc., Billerica, MA 01821; [l]Department of Chemistry, Faculty of Science, University of Helsinki, 00014 Helsinki, Finland; [m]Aerosol and Haze Laboratory, Beijing Advanced Innovation Center for Soft Matter Science and Engineering, Beijing University of Chemical Technology, 100089 Beijing, China; and [n]Joint International Research Laboratory of Atmospheric and Earth System Sciences, Nanjing University, 210023 Nanjing, China

Edited by Mark Thiemens, University of California San Diego, La Jolla, CA, and approved December 10, 2020 (received for review May 18, 2020)

Reactive iodine plays a key role in determining the oxidation capacity, or cleansing capacity, of the atmosphere in addition to being implicated in the formation of new particles in the marine boundary layer. The postulation that heterogeneous cycling of reactive iodine on aerosols may significantly influence the lifetime of ozone in the troposphere not only remains poorly understood but also heretofore has never been observed or quantified in the field. Here, we report direct ambient observations of hypoiodous acid (HOI) and heterogeneous recycling of interhalogen product species (i.e., iodine monochloride [ICl] and iodine monobromide [IBr]) in a midlatitude coastal environment. Significant levels of ICl and IBr with mean daily maxima of 4.3 and 3.0 parts per trillion by volume (1-min average), respectively, have been observed throughout the campaign. We show that the heterogeneous reaction of HOI on marine aerosol and subsequent production of iodine interhalogens are much faster than previously thought. These results indicate that the fast formation of iodine interhalogens, together with their rapid photolysis, results in more efficient recycling of atomic iodine than currently considered in models. Photolysis of the observed ICl and IBr leads to a 32% increase in the daytime average of atomic iodine production rate, thereby enhancing the average daytime iodine-catalyzed ozone loss rate by 10 to 20%. Our findings provide direct field evidence that the autocatalytic mechanism of iodine release from marine aerosol is important in the atmosphere and can have significant impacts on atmospheric oxidation capacity.

iodine | heterogeneous reaction | halogen recycling | ozone loss

Halogen chemistry has been known to deplete both stratospheric and tropospheric ozone (1, 2) and initiate new particle formation in the marine atmosphere (3, 4). Field studies have shown the widespread presence of halogen atoms and oxides in different environments (5, 6). Recent findings of the threefold increase of atmospheric iodine levels in the Arctic and Europe over the past 50 y (7, 8) indicate that the concurrent environmental changes have triggered an increase in iodine emissions, thus enhancing all iodine-associated impacts in the atmosphere. Tropospheric iodine is also projected to increase throughout the 21st century with important implications for tropospheric ozone and air quality (9). A key uncertainty in assessing the global impact of tropospheric iodine is the occurrence and efficiency of heterogeneous recycling reactions of iodine species on aerosol surfaces. Two decades ago, Vogt et al. (10, 11) proposed a theoretical mechanism for halogen recycling via heterogeneous uptake of hypoiodous acid (HOI) onto sea-salt aerosol particles to produce the iodine interhalogen species (e.g., iodine monochloride [ICl] and iodine monobromide [IBr]), which upon photolysis rapidly release highly reactive halogen atoms (I, Br, and Cl). Although laboratory studies have demonstrated that the heterogeneous uptake of HOI onto chloride- and bromide-containing aerosol surfaces and freezing of the

Significance

Recycling of reactive iodine from heterogeneous processes on sea-salt aerosol was hypothesized over two decades ago to play an important role in the atmospheric cleansing capacity. However, the understanding of this mechanism has been limited to laboratory studies and has not been confirmed in the atmosphere until now. We present atmospheric measurement of gas-phase iodine interhalogen species and show that their production via heterogeneous processing on marine aerosols is remarkably fast. These observations reveal that the atmospheric recycling of atomic iodine through photolysis of iodine interhalogen species is more efficient than previously thought, which is ultimately expected to lead to higher ozone loss and faster new particle formation in the marine environment.

Author contributions: Y.J.T., A.S.-L., and M.S. designed research; Y.J.T., X.-C.H., J.S., J.K., T.L., S.J., L.B., D.K., M.O., N.S., J.M., J.H., M.M., L.Y., Y.W., D.W., Q.Z., J.V., T.G.S., S.O., R.L.M., J.O., D.C., N.M.M., M.D.M., and M.S. performed research; Y.J.T., Q.L., C.A.C., S.I., and A.S.-L. contributed new reagents/analytic tools; Y.J.T., X.-C.H., Q.L., J.S., J.K., C.Y., S.I., T.L., N.S., J.O., D.C., N.M.M., M.D.M., and A.S.-L. analyzed data; and Y.J.T., X.-C.H., Q.L., C.A.C., C.Y., S.I., R.C.T., H.L., W.H., Y.W., J.V., T.J., F.B., T.P., D.R.W., R.L.M., J.O., D.C., N.M.M., M.K., C.O., M.D.M., A.S.-L., and M.S. wrote the paper.

The authors declare no competing interest.

This article is a PNAS Direct Submission.

[1]Present address: School of Marine Sciences, Sun Yat-Sen University, 519082 Zhuhai, China.

[2]To whom correspondence may be addressed. Email: a.saiz@csic.es or mikko.sipila@helsinki.fi.

This article contains supporting information online at https://www.pnas.org/lookup/suppl/doi:10.1073/pnas.2009951118/-/DCSupplemental.

Published January 21, 2021.

halide-rich solution can lead to the formation of ICl and IBr (12–14), such mechanism has so far not been confirmed in the ambient atmosphere.

HOI at Mace Head

Direct observations of HOI, ICl, and IBr in the atmosphere have never been demonstrated. In this study, we conducted an intensive measurement campaign at Mace Head with a newly developed bromide-based chemical ionization atmospheric pressure interface time-of-flight mass spectrometer (Br-CI-APi-TOF), which enabled us to measure HOI, ICl, and IBr simultaneously with high resolution (*Materials and Methods*). HOI shows a clear diurnal pattern during the entire measurement period with highest mixing ratios at low tide (Fig. 1*A*), reaching a maximum of 66.6 parts per trillion by volume (pptv). The concentrations of HOI are strongly correlated with those of molecular iodine (I_2) in the daytime and precisely track the solar radiation profile (Fig. 1*B*). On the contrary, low levels of HOI (close to the limit of detection) are measured during the nighttime low-tide events, despite the presence of remarkably high mixing ratios of I_2, up to 256 pptv. It is well known that the high concentrations of I_2 during low tides are associated with the emission from the exposed macroalgae bed in the region (15–18), but an interesting question arising here is the source of elevated levels of HOI measured at Mace Head.

Fig. 1*C* depicts the ratio of HOI to I_2 during the campaign (5-min average), with typical values of less than 1 and a maximum value of 2. The daytime maxima of HOI to I_2 ratio during the high tide (tide height $\geq$ 2 m) over the entire campaign ranged from 0.006 to 2.0, while during low tide (tide height < 2 m), the range was 0.002 to 1.6. The relatively smaller ratios during low-tide events ($P < 0.01$) are due to the higher emission of I_2 from exposed macroalgae beds as water recedes. Direct emission of HOI from macroalgae is likely small, given that the stress-induced production of reactive oxygen species such as hydrogen peroxide (H_2O_2) inside the macroalgae converts most HOI into iodide (I^-) and I_2 prior to its release to the atmosphere (19–21). This is supported by the observed HOI to I_2 ratio being near zero during the nocturnal low tides. Another possible source of HOI is the O_3 deposition onto the iodide-containing seawater (22). However, the HOI to I_2 ratios observed in this study are lower than those reported in the laboratory experiments (22). Notably, the HOI concentrations (e.g., from June 27 to July 2) are low despite the hourly average O_3 concentrations being higher than 40 parts per billion by volume (ppbv), clearly suggesting that the O_3 deposition mechanism is not a controlling factor for the measured HOI at Mace Head. Another factor that may contribute to the relatively low HOI to I_2 ratios recorded during the high O_3 period is the enhancement of nitrogen oxides (*SI Appendix*, Fig. S1) which can reroute the iodine oxides to produce iodine nitrate ($IONO_2$) via Eq. **4** instead of HOI formation

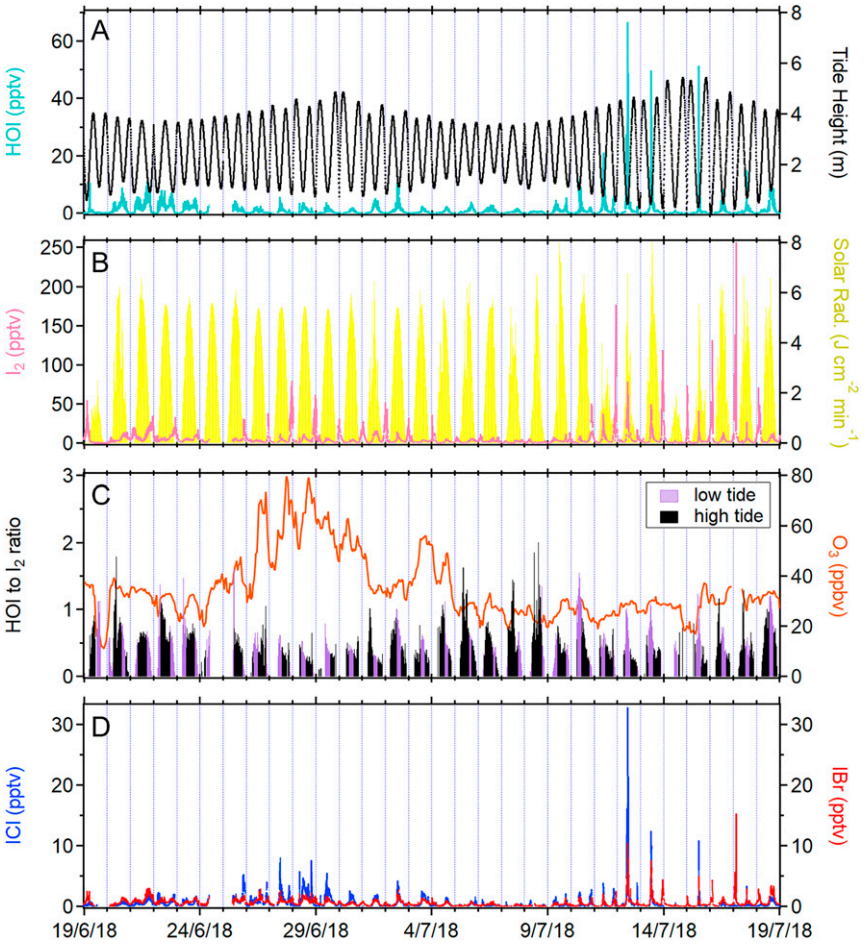

Fig. 1. Time series of (*A*) HOI and the tidal heights and (*B*) I_2 and solar radiation at Mace Head Observatory from June 19 to July 19, 2018 (1-min average data). (*C*) The ratio of HOI to I_2 mixing ratios (5-min average) in relation to the O_3 concentration. The I_2 and HOI mixing ratios below the detection and quantification were omitted. The ozone data are 1-h average. (*D*) Time series of ICl and IBr observed during the campaign (1-min average). The time presented in this study is in Coordinated Universal Time (+1 in local time).

(Eq. **3**). Based on these observations, we can conclude that the daytime HOI at Mace Head is predominantly produced via photochemical reactions initiated by the algae emissions of I_2 (i.e., Eq. **1** to Eq. **3**).

$$I_2 + h\nu \rightarrow 2I \quad [1]$$

$$I + O_3 \rightarrow IO + O_2 \quad [2]$$

$$IO + HO_2 \rightarrow HOI + O_2 \quad [3]$$

$$IO + NO_2 \rightarrow IONO_2 \quad [4]$$

Observation of ICl and IBr

Besides photolysis, the other important loss pathway of HOI is its heterogeneous uptake onto halide-rich aerosol surfaces to produce interhalogens ICl and IBr (12, 13). We measured significant levels of ICl and IBr throughout the measurement period, with mean daily maxima of 4.3 ± 6 pptv and 3.0 ± 3 pptv (mean ± SD), respectively. The concentrations for both species peak during the low tide, coinciding with elevated levels of I_2 (Fig. 1*D* and *SI Appendix*, Fig. S2*A*), which is in agreement with a previous offline measurement of activated iodine compounds (HOI+ICl) that also showed a strong correlation with I_2 (23).

A study in La Jolla, California reported that concentrations of ICl and IBr were below detection limits of 0.5 and 0.4 pptv (24). In our measurements, the observed daytime levels of ICl and IBr generally have good positive correlations with both HOI and I_2 concentrations (their correlation coefficients, $r \geq 0.67$; $P < 0.01$). They also display a positive relationship with the production rate of atomic iodine (I), calculated from the photolysis of I_2 (Eq. **1**) and O_3 concentration during the daytime (Fig. 2*A*). These positive relationships show that the increase in the photochemical production of HOI (i.e., via reactions Eq. **1** to Eq. **3**) is coupled to the production of ICl and IBr. We also find that ICl and IBr generally increase with the aerosol surface area at a given HOI concentration (Fig. 2*B* and *SI Appendix*, Fig. S3) and closely follow the variations of particulate iodide (*SI Appendix*, Fig. S4). These evidences, along with the fact that the heterogeneous processing of HOI and $IONO_2$ on particulate chloride or bromide (Eqs. **5** and **6**), are the main production pathways to form ICl and IBr in the marine atmosphere (5), strongly suggest that the heterogeneous reaction of HOI on aerosol (Eq. **5**) is the major source of ICl and IBr at Mace Head. The formation pathway through Eq. **6** is expected to be less important during

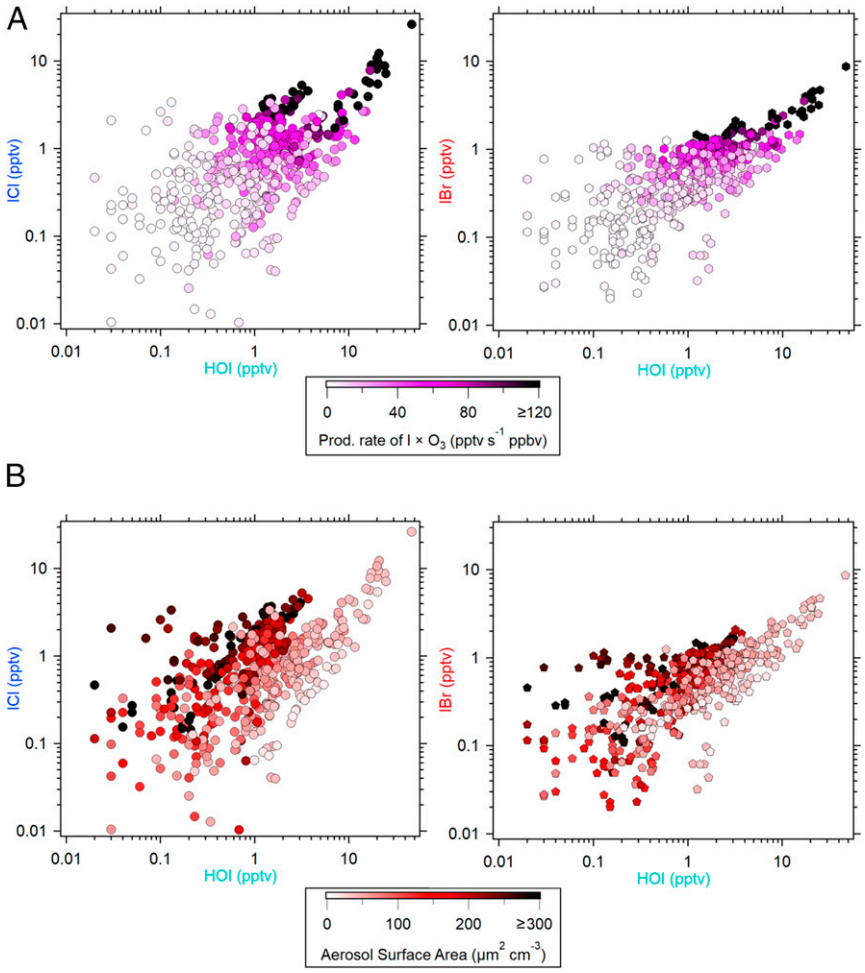

Fig. 2. Log-scale scatter plots of HOI (*x*-axis) versus ICl and IBr (*y*-axis) showing (*A*) their relationships with atomic I production rate (calculated from the photolysis of I_2) multiplied by O_3 concentration (color-coded) and (*B*) their relationships with aerosol surface area (color-coded). Notable mixing ratios of ICl and IBr (above their instrument LOD of 0.15 and 0.08 pptv, respectively) can be observed when HOI is above 0.1 pptv (instrument LOD for HOI is 0.09 pptv). For this analysis, only data at daytime low tides (tidal height < 2 m and solar radiation > 0 J · cm^{-2} · min^{-1}) from June 26 to July 14 of 2018 were used. Refer to *SI Appendix*, Fig. S5 for nighttime data.

the daytime due to the shorter photolysis lifetime of $IONO_2$ (~20 s at noontime) in comparison with that of HOI (~110 s at noontime). Note that although ICl and IBr can also be formed via the gas-phase reactions of IO+ClO and IO+BrO, respectively, the calculated rate of gas-phase production for typical levels of halogen oxides measured at Mace Head (25, 26) is at least 40 times slower than the heterogeneous production of ICl and IBr via the reaction of HOI on aerosol (*SI Appendix*, section S6):

$$HOI + Cl^{-} or\ Br^{-} \rightarrow ICl\ or\ IBr \quad [5]$$

$$IONO_2 + Cl^{-} or\ Br^{-} \rightarrow ICl\ or\ IBr \quad [6]$$

Therefore, these results indicate active iodine chemistry in the aerosol-phase, with HOI uptake being a controlling factor of daytime aerosol–iodine processing via reaction with chloride/bromide. The concentration difference between ICl and IBr is likely caused by the availability of bromide in the aerosol since the production of IBr dominates in the presence of bromide (12). Over time, the aerosol can become bromide depleted (27, 28), while the chloride level is not considered to be a limiting factor for reactions Eqs. **5** and **6**, at least in the coastal marine boundary layer.

As shown in Fig. 1*D* and *SI Appendix*, Fig. S2*A*, the interhalogens typically peak at daytime low tide. However, there are also enhancements of ICl and IBr concentrations during the nighttime low tides. Similar to the daytime, the nocturnal observations of ICl and IBr also coincide with high I_2 and high aerosol surface area despite the very low HOI concentrations (see example in the green shaded area in *SI Appendix*, Fig. S2*A*). This observation indicates that HOI processing on aerosol is not the dominant source of interhalogens at night. The increase of ICl and IBr after sunset is likely due to the oxidation reaction of I_2 by the nitrate radical (NO_3), leading to the production of $IONO_2$ via Eq. **7**, which subsequently undergoes heterogeneous reaction with marine aerosol (see Eq. **6**) to form ICl and IBr (16, 29–32):

$$I_2 + NO_3 \rightarrow I + IONO_2. \quad [7]$$

Our analysis suggests that I_2, aerosol surface area, and the precursors of NO_3 (i.e., ozone and nitrogen oxides [NO_x]) likely have a significant influence on the level of nighttime ICl and IBr. Detectable levels of nocturnal IBr and ICl are associated with increases in ozone, nitric acid (HNO_3, a proxy of NO_x), and aerosol surface area (*SI Appendix*, Fig. S5). Note that I_2 is also emitted during the nighttime low tides (typically in the range of 1 to 100 pptv) and its nocturnal lifetime is much longer than that during daytime when it undergoes rapid photolysis. Previous measurements at Mace Head have reported that the NO_3 radical is always present after sunset with mixing ratios ranging from several to tens of pptv (25, 33). Furthermore, our calculation with an explicit Tropospheric Halogen Chemistry Model, THAMO (*Materials and Methods*), shows that $IONO_2$ levels are higher at night (*SI Appendix*, Fig. S6). A sensitivity test was performed by increasing the nitrogen oxides concentration (an important precursor of $IONO_2$; refer to Eq. **4** and Eq. **7**) twofold, which leads to a sharp increase in $IONO_2$ mixing ratios during the nighttime low-tide events, while no significant changes are observed during the daytime. Hence, our results indicate that the heterogeneous reaction of HOI is a major daytime source of ICl and IBr, while $IONO_2$ is the most likely source of the iodine interhalogen species at night.

Heterogeneous Production of ICl and IBr

The heterogeneous uptake of HOI and the subsequent production of iodine interhalogens can be rapid (12, 30, 34). Analogous to hypobromous acid (HOBr), the HOI reactive uptake on the aerosol is likely accommodation limited under ambient conditions (35). We constrained the THAMO model with the observations of I_2, HOI, aerosol surface area, O_3, and relevant meteorological parameters to evaluate the production of iodine interhalogens. Fig. 3*A* illustrates the diel pattern comparison between the observed and modeled concentrations of ICl and IBr derived from different heterogeneous uptake coefficients (γ), along with their uncertainty range. We find a remarkable difference between the observed and modeled iodine interhalogen concentrations when adopting a γ of 0.1 for HOI, a lower-limit value recommended by the International Union of Pure and Applied Chemistry kinetic database (36), assuming that this reactive uptake is accommodation limited. As a result, the model concentrations of ICl and IBr are significantly underestimated, on average reproducing only ~10 ± 6% (mean ± upper and lower limit) of the observed daytime mean concentrations. For γ of 0.3, the model is able to reproduce ~26 ± 17% of the daytime observations. An upper limit of γ of 0.9 is needed to reproduce the majority (~68 ± 43%) of the daytime mean concentrations of ICl and IBr, which is within the uncertainty range of the observations and simulations (Fig. 3*A*). Note that the remaining fractions of the observed ICl and IBr could also be contributed by the heterogeneous reaction of other halogen acids such as HOBr and hypochlorous acid, HOCl, and the heterogeneous oxidation of aerosol particles by gas-phase radicals such as OH, Cl, and Br (25, 35, 37, 38). This analysis suggests that a rapid HOI heterogeneous uptake is required to explain the observed ICl and IBr. Previous laboratory studies reported γ values from 0.002 to 0.061 for HOI uptake on sea-salt films and wetted-wall halides under laboratory conditions (*SI Appendix*, Table S1) (12, 13, 30). The discrepancy between the uptake coefficients inferred from our observations and those derived in laboratory studies could be due to many factors including the different chemical compositions, mixtures, and morphology of the aerosol, highlighting the complex role of ambient aerosols in the heterogeneous uptake of HOI.

We now evaluate the influence of the aerosol chemical composition on the rapid heterogeneous production of ICl and IBr. We observe that the increase in sulfate aerosol (SO_4^{2-}) concentration leads to an enhancement of the intercept of the plot of iodine interhalogens versus HOI concentrations (Fig. 3*B*). This observation indicates that higher aerosol sulfate reduces the aerosol pH, leading to a faster production of ICl and IBr since acidic aerosol particles promote the heterogeneous uptake of halogen species (39). Holmes et al. (30) reported a lower-limit coefficient of 0.3 for HOI accommodation on the H_2SO_4 surface at 253 °K, suggesting that the heterogeneous uptake of HOI could be larger than 0.3 under acidic aerosol conditions. In agreement, our analysis shows that in order to reproduce the observations, the HOI uptake coefficient needs to be >0.3, in line with the fact that typical marine aerosol is acidic (40, 41). Overall, our results reveal that the observed heterogeneous production of iodine interhalogens is faster than expected by current knowledge. As a consequence, the currently implemented HOI uptake value of ≤0.1 in global atmospheric models (42, 43) may largely underestimate the global production of these iodine interhalogen species.

Atmospheric Impacts of ICl and IBr

Photolysis of ICl and IBr rapidly releases reactive halogen atoms which significantly affect atmospheric oxidizing capacity. We estimate that the photolysis of the observed ICl and IBr results in a daytime average atomic I production rate of 0.03 ± 0.06 pptv · s^{-1} (mean ± SD). Fig. 4*A* illustrates the relative changes of modeled total atomic I production rate with and without consideration of the measured IBr and ICl. A significant increase of atomic I production, with a daytime (05:00 to 21:00) mean of 32 ± 19% (mean ± SD), is calculated when considering the

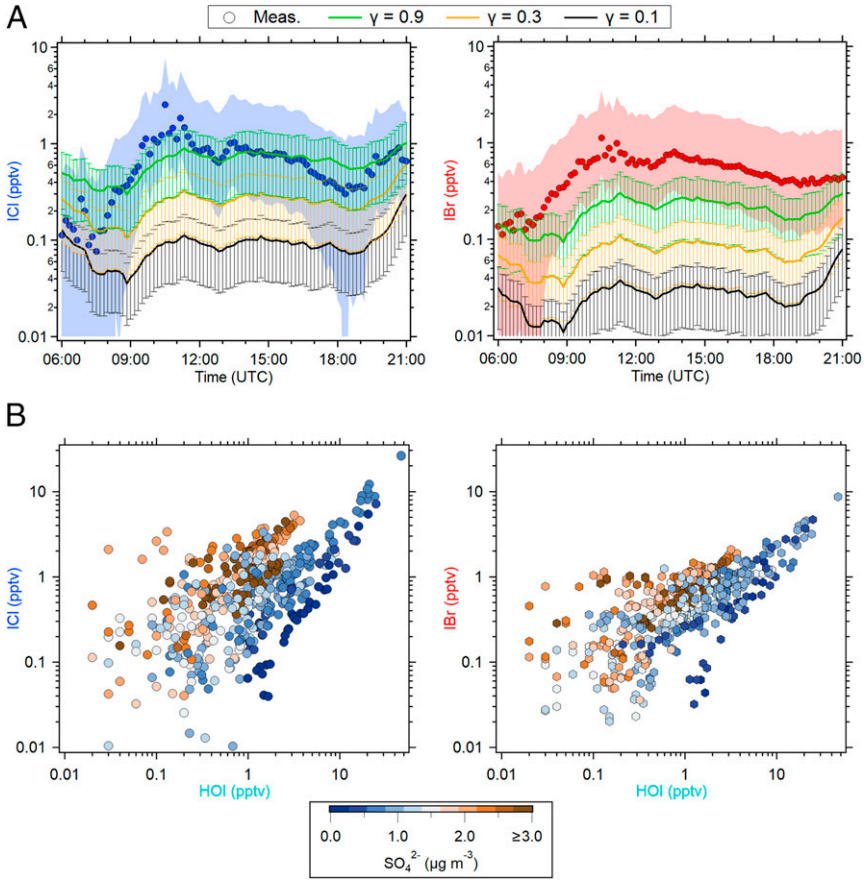

Fig. 3. (*A*) Diel pattern of the observed versus modeled ICl and IBr during daytime. The solid circle represents the average value of ambient observation of ICl (blue) and IBr (red). The shaded area is the uncertainty for ICl and IBr measurements (±200% + LOD). Error bar shows the estimated uncertainty for the simulations (±63%), calculated using the propagation of uncertainties of HOI measurement and aerosol surface area. The data from June 26 to July 14 of 2018 were used in this analysis due to the availability of continuous data for use in THAMO modeling. (*B*) The three-way relationships of aerosol-sulfate concentration with ICl and IBr, together with HOI. The aerosol-sulfate concentration was measured by the aerosol mass spectrometer which has an inlet with particle cutoff of 1 μm in size (refer to *SI Appendix*, Table S4). Note that only data at daytime low tides (tidal height < 2 m and solar radiation > 0 J · cm^{-2} · min^{-1}) from June 26 to July 14 of 2018 were used.

observed ICl and IBr. The contribution of different species to the average production rate of iodine atoms is depicted in Fig. 4*B*. It can be seen that the photolysis of I_2, iodine monoxide (IO), and iodine dioxide (OIO) are the dominant sources of atomic I, while the direct contributions from HOI and $IONO_2$ photolysis to the total atomic I production rate are small. The direct photolysis of ICl and IBr only accounts for about 2% of the total atomic I production. However, the inclusion of the iodine interhalogens significantly increases the concentrations of iodine oxides such as IO and OIO, and their photolysis subsequently leads to a larger (32 ± 19%) total atomic I production. This result suggests that atomic I recycled from the ICl and IBr photolysis is rapidly oxidized and converted into other iodine oxides. In other words, the heterogeneous production of ICl and IBr is a source for daytime IO and would be an important process to sustain the elevated IO in the atmosphere as detected in coastal and open-ocean environments (44–47). Note that previous work reported that I_2 and iodocarbons emissions were insufficient to explain the observed 1 to 2 pptv IO levels at Cape Verde and suggested that an additional unknown source of inorganic iodine was necessary to account for the IO observations (46). Thus, our findings link to such missing source of reactive iodine at Cape Verde (46) and demonstrate that the existence of HOI in the atmosphere can lead to a faster-than-anticipated formation of ICl and IBr, and their rapid photolysis lifetime significantly accelerates the recycling of iodine in the atmosphere.

We now turn to the impact of ICl and IBr on O_3 loss at Mace Head. Previous studies show that iodine-catalyzed chemistry can lead to about 13 to 20% of total integrated O_3 loss in the global troposphere (43, 48–50). Fig. 4*C* shows the comparison of the iodine-catalyzed O_3 loss rate with and without the photolysis of observed interhalogens. The model estimates a daily average O_3 loss rate up to 21 ppbv · h^{-1} and 24 ppbv · h^{-1} without and with inclusion of the rapid photolysis of ICl and IBr, respectively. The average daytime ozone loss rate is enhanced by about 12% and up to 86% in individual cases (*SI Appendix*, Fig. S7), demonstrating that the observed fast production of iodine interhalogens could ultimately lead to higher ozone loss than previously predicted by conventional iodine chemistry.

In addition to O_3 loss, the enhanced formation of IO_x (I + IO) via fast recycling of ICl and IBr could accelerate iodine-driven new particle formation. The IO_x undergoes a chain reaction to form higher iodine oxides (I_xO_y) and iodic acid (HIO_3), both being potential precursors of new particles. O'Dowd and coworkers (3) demonstrated that new particles can be produced from condensable iodine-containing vapors. Recent studies (4, 51) identified that the cluster formation was sustained by sequential addition of HIO_3, and although the formation mechanism of HIO_3 is still unclear (52), the elevated HIO_3 is strongly linked to the photochemistry of IO_x. Indeed, the observations of ultrafine particle concentrations in coastal locations are strongly correlated with the rapid processing of IO (53). Therefore, the

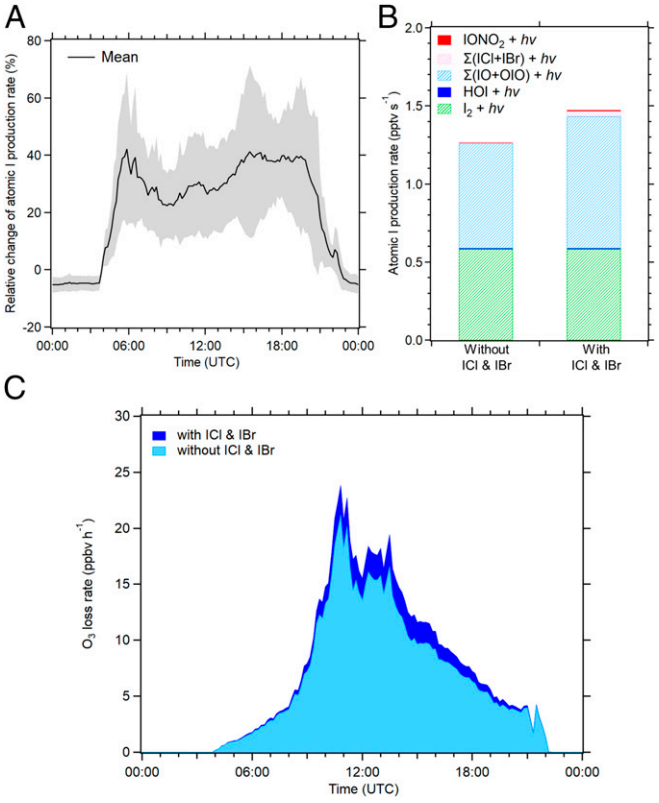

Fig. 4. (*A*) Changes in atomic I production rates between the simulations with and without constraining ICl and IBr. The black solid line is the mean value and the gray shaded area is the ±SD. (*B*) The daytime average atomic I production rates from photolysis of different iodine species under conditions with and without ICl and IBr. (*C*) The O_3 loss rates modeled with and without ICl and IBr. Note that this figure is based on data from June 26 to July 14 of 2018 as indicated in the model description (*SI Appendix*, section S5). The data are averaged over 10-min intervals.

observed high levels of ICl and IBr can promote the fast production of precursors of iodine-mediated particles, leading to enhanced new particle formation, which potentially grow to cloud condensation nuclei in the marine environment (3, 4, 54).

The photolysis of ICl and IBr is also a source of atomic chlorine (Cl) and bromine (Br). We calculate that their photolysis results in an average daytime production rate of Cl and Br of 0.01 and 0.02 pptv · s^{-1}, respectively (*SI Appendix*, Fig. S8). With the assumption that the lifetime of atomic Cl and Br at Mace Head is being regulated by the reaction with ozone (average daytime O_3 of 38.7 ppbv), photolysis of ICl and IBr would lead to a daytime average steady-state concentration of atomic Cl and Br of ~10^4 and ~10^5 molecule cm^{-3}. This additional source of atomic halogen radicals is likely to have a significant influence on the oxidation processes in the marine atmosphere (*SI Appendix*, Fig. S9).

A final point to consider is the potential occurrence of iodine interhalogens in the global marine boundary layer. From the observations at Mace Head, we show that efficient HOI heterogeneous uptake and further processing is a controlling factor for the production of higher-than-expected levels of ICl and IBr. We observe that ICl and IBr are above the instrument detection limit when HOI is >0.1 pptv (refer to Fig. 2*B*). The HOI concentration needed for the discernible iodine interhalogen production could be lower when the aerosol surface area is larger. Mace Head is known to be a hotspot for iodine chemistry, and the question arising here is whether this fast heterogeneous production of ICl and IBr could take place in other marine environments. To explore this potential implication, we compare our observations with previous marine iodine measurements at La Jolla and Cape Verde that reported an average of 0.7 pptv of I_2 (La Jolla) and daytime upper limits of I_2 in the range of ~0.4 to 1.2 pptv (Cape Verde), while the concentrations of ICl and IBr were below the detection limits at both places (24, 46). With these levels of daytime I_2 (i.e., in range 0.4 to 1.2 pptv), the average daytime low-tide ICl and IBr mixing ratios from our observation at Mace Head were 0.46 (±0.2) pptv and 0.25 (±0.2) pptv, respectively (*SI Appendix*, Fig. S10). These values are coincidently below the detection limits of 0.5 pptv (for ICl) and 0.4 pptv (for IBr) at La Jolla and Cape Verde, as originally reported by Finley and Saltzman (24). In a separate modeling study, McFiggans et al. (55) estimated negligible levels of daytime ICl and IBr at Mace Head and Cape Grim (Australia) for an HOI uptake coefficient of 0.02. However, if the HOI uptake coefficient was increased in their calculation (e.g., $\gamma \geq 0.3$), noticeable levels (up to 0.9 pptv) of daytime ICl and IBr could then be predicted both at Mace Head and Cape Grim (*SI Appendix*, section S7), which are within the range of our ICl and IBr observations (*SI Appendix*, Fig. S11). This also shows that earlier models could indeed simulate significant daytime levels of ICl and IBr if the HOI heterogeneous uptake coefficient is ≥0.3. These comparisons indicate that the observed rate of ICl and IBr production via HOI heterogeneous uptake at Mace Head is a fundamental process that can take place over the open ocean, albeit at likely lower concentrations than at Mace Head. Furthermore, laboratory experiments have reported that the O_3 deposition onto the ocean surface can lead to daytime emission of ~7×10^7 molecule of HOI · cm^{-2} · s^{-1} (22, 56). Based on this mechanism, recent models predict that a significant amount of HOI (in the range of ~2 to 15 pptv) is potentially spreading over the global marine boundary layer (43, 57, 58). This worldwide ocean emission of HOI would be sufficient to activate significant widespread ICl and IBr production. Therefore, although open-ocean measurements of HOI, ICl, and IBr are sorely needed, our findings, along with previous field and laboratory iodine measurements, suggest that the fast heterogeneous activation of ICl and IBr is likely ubiquitous in the global marine atmosphere.

Our study reveals observational evidence of significant levels of HOI, ICl, and IBr in the North Atlantic coastal environment following the theoretical proposal of Vogt et al. (10, 11) suggested over 20 y ago. Remarkably, the observed iodine-heterogeneous recycling can occur at much faster rates than theoretically proposed and currently implemented in models. Further laboratory and field studies are required to understand the factors that contribute to the fast heterogeneous uptake of HOI and production of ICl and IBr. However, these findings indicate that the efficient heterogeneous recycling of iodine can be important in the marine atmosphere and can have significant impacts on iodine-catalyzed ozone loss and new particle formation in the troposphere.

Materials and Methods

Measurements. We conducted in situ measurements at Mace Head Observatory in Ireland (53°19′ N, 9°54′ W) from June 19 to July 19, 2018, to study iodine-heterogeneous chemistry. Br-CI-APi-TOF was deployed to measure I_2, HOI, ICl, and IBr. We performed postcampaign calibrations for I_2 and HOI and estimated the calibration coefficients of ICl and IBr via quantum chemical calculations and based on the calibration coefficients obtained from I_2, HOI, sulfuric acid (H_2SO_4), and molecular chlorine (Cl_2) calibrations. The ambient humidity is expected to have minor effects on our measurements of I_2, HOI, ICl, and IBr due to the inclusion of the data normalization with the sum of bromide ions and bromide water cluster (*SI Appendix*, Eq. S1). The limits of detection (LOD) were determined to be 0.09, 0.15, 0.08, and 0.07 pptv (1-min average, 3 σ) for HOI, ICl, IBr, and I_2, respectively. The total uncertainty for the detection of I_2 and HOI was estimated to be ± 45 and 55%, respectively, while for ICl and IBr, a factor of two (±200% + LOD) was predicted. Note that the reported measurement uncertainties of HOI, ICl, IBr, and I_2 at Mace Head can be considered as lower limits due to the lack of in-field calibrations. This study was also facilitated by the other gas-phase,

aerosol-phase, and meteorological measurements available in the observatory. The aerosol surface area was estimated with information obtained from the size-distribution measurements and the particulate matter–mass observations (refer to *SI Appendix*, sections S1–S4 for a more detailed description of the site, instrumentation, measurement and calibration methods, and calculation of aerosol surface area).

Modeling. THAMO, documented in detail in Saiz-Lopez et al. (59), was used to calculate the $IONO_2$ concentration and production of ICl and IBr. The model was constrained by the observed I_2, HOI, IBr, ICl, and other relevant chemical and meteorological parameters. We also used THAMO to assess the impact of ICl and IBr on the O_3 loss rate. The detail description on the model setup can be found in *SI Appendix*, section S5. Details on the calculation of the production rate of ICl and IBr via heterogeneous process of HOI and gas-phase reactions can be found in *SI Appendix*, section S6. *SI Appendix*, section S7 describes the calculation of daytime steady-state concentrations of ICl and IBr.

Data Availability. All study data are included in the article and/or *SI Appendix*. Data related to this article are also available in Zenodo at https://doi.org/10.5281/zenodo.4438584.

ACKNOWLEDGMENTS. We acknowledge financial support from the Academy of Finland (3282290, 306853, 296628, 310626, 315203, 311932, 299574, 326437, 307537, 316114, and 326948), Jane and Aatos Erkko Foundation, European Research Council Executive Agency under the European Union's Horizon 2020 Research and Innovation Programme (Project ERC-2016-COG 726349 CLIMAHAL), European Research Council (GASPARCON, grant 714621), European Research Council via Atmospheric Gas-to-Particle conversion (ATM-GTP) 266 (grant 742206), H2020 European Research Council (grant CHAPAs [850614]), and the Aerosol, Clouds and Trace Gases Research Infrastructure 2—Trans-National Access Consistent Consistent and Mobile Direct Observation of Cluster Formation in Diverse European Environmental Zones: Mace Head (ACTRIS-2 TNA CONDENZ:MHD) from the European Union's Horizon 2020 Research and Innovation Programme under grant agreement No. 654109. We would also like to acknowledge the Mace Head operational support from the EPA-Ireland, Department of Communications, Climate Action and Environment and contributions from COST Action CA16109 (COLOSSAL), MaREI, and the SFI Research Centre for Energy, Climate and Marine. M.O. and J.K. wish to thank the doctoral school of the Faculty of Engineering and Natural Science. We thank Professor Joel A. Thornton for the scientific discussion and Valtteri Suorsa and Heini Ali-Kovero for assisting with the experiment.

1. M. J. Molina, F. S. Rowland, Stratospheric sink for chlorofluoromethanes: Chlorine atom-catalysed destruction of ozone. *Nature* **249**, 810–812 (1974).
2. L. A. Barrie, J. W. Bottenheim, R. C. Schnell, P. J. Crutzen, R. A. Rasmussen, Ozone destruction and photochemical reactions at polar sunrise in the lower Arctic atmosphere. *Nature* **334**, 138–141 (1988).
3. C. D. O'Dowd *et al*., Marine aerosol formation from biogenic iodine emissions. *Nature* **417**, 632–636 (2002).
4. M. Sipilä *et al*., Molecular-scale evidence of aerosol particle formation via sequential addition of HIO_3. *Nature* **537**, 532–534 (2016).
5. A. Saiz-Lopez, R. von Glasow, Reactive halogen chemistry in the troposphere. *Chem. Soc. Rev.* **41**, 6448–6472 (2012).
6. W. R. Simpson, S. S. Brown, A. Saiz-Lopez, J. A. Thornton, Rv. Glasow, Tropospheric halogen chemistry: Sources, cycling, and impacts. *Chem. Rev.* **115**, 4035–4062 (2015).
7. C. A. Cuevas *et al*., Rapid increase in atmospheric iodine levels in the North Atlantic since the mid-20th century. *Nat. Commun.* **9**, 1452 (2018).
8. M. Legrand *et al*., Alpine ice evidence of a three-fold increase in atmospheric iodine deposition since 1950 in Europe due to increasing oceanic emissions. *Proc. Natl. Acad. Sci. U.S.A.* **115**, 12136–12141 (2018).
9. F. Iglesias-Suarez *et al*., Natural halogens buffer tropospheric ozone in a changing climate. *Nat. Clim. Chang.* **10**, 147–154 (2020).
10. R. Vogt, P. J. Crutzen, R. Sander, A mechanism for halogen release from sea-salt aerosol in the remote marine boundary layer. *Nature* **383**, 327–330 (1996).
11. R. Vogt, R. Sander, R. von Glasow, P. J. Crutzen, Iodine chemistry and its role in halogen activation and ozone loss in the marine boundary layer: A model study. *J. Atmos. Chem.* **32**, 375–395 (1999).
12. C. F. Braban *et al*., Heterogeneous reactions of HOI, ICl and IBr on sea salt and sea salt proxies. *Phys. Chem. Chem. Phys.* **9**, 3136–3148 (2007).
13. J. C. Mössinger, R. A. Cox, Heterogeneous reaction of HOI with sodium halide salts. *J. Phys. Chem. A* **105**, 5165–5177 (2001).
14. D. O'Sullivan, J. R. Sodeau, Freeze-induced reactions: formation of iodine-bromine interhalogen species from aqueous halide ion solutions. *J. Phys. Chem. A* **114**, 12208–12215 (2010).
15. G. McFiggans *et al*., Direct evidence for coastal iodine particles from *Laminaria* macroalgae – linkage to emissions of molecular iodine. *Atmos. Chem. Phys.* **4**, 701–713 (2004).
16. A. Saiz-Lopez, J. M. C. Plane, Novel iodine chemistry in the marine boundary layer. *Geophys. Res. Lett.* **31**, L04112 (2004).
17. A. Saiz-Lopez *et al*., Modelling molecular iodine emissions in a coastal marine environment: The link to new particle formation. *Atmos. Chem. Phys.* **6**, 883–895 (2006).
18. D. E. Heard *et al*., The North Atlantic marine boundary layer experiment (NAMBLEX). Overview of the campaign held at Mace Head, Ireland, in summer 2002. *Atmos. Chem. Phys.* **6**, 2241–2272 (2006).
19. F. C. Küpper *et al*., Iodide accumulation provides kelp with an inorganic antioxidant impacting atmospheric chemistry. *Proc. Natl. Acad. Sci. U.S.A.* **105**, 6954–6958 (2008).
20. F. C. Küpper *et al*., Iodine uptake in Laminariales involves extracellular, haloperoxidase-mediated oxidation of iodide. *Planta* **207**, 163–171 (1998).
21. S. Dixneuf, A. A. Ruth, S. Vaughan, R. M. Varma, J. Orphal, The time dependence of molecular iodine emission from Laminaria digitata. *Atmos. Chem. Phys.* **9**, 823–829 (2009).
22. L. J. Carpenter *et al*., Atmospheric iodine levels influenced by sea surface emissions of inorganic iodine. *Nat. Geosci.* **6**, 108–111 (2013).
23. R.-J. Huang, T. Hoffmann, Development of a coupled diffusion denuder system combined with gas chromatography/mass spectrometry for the separation and quantification of molecular iodine and the activated iodine compounds iodine monochloride and hypoiodous acid in the marine atmosphere. *Anal. Chem.* **81**, 1777–1783 (2009).
24. B. D. Finley, E. S. Saltzman, Observations of Cl_2, Br_2, and I_2 in coastal marine air. *J. Geophys. Res. Atmos.* **113**, D21301 (2008).
25. A. Saiz-Lopez, J. A. Shillito, H. Coe, J. M. C. Plane, Measurements and modelling of I_2, IO, OIO, BrO and NO_3 in the mid-latitude marine boundary layer. *Atmos. Chem. Phys.* **6**, 1513–1528 (2006).
26. A. Saiz-Lopez, J. M. C. Plane, J. A. Shillito, Bromine oxide in the mid-latitude marine boundary layer. *Geophys. Res. Lett.* **31**, L03111 (2004).
27. G. P. Ayers, R. W. Gillett, J. M. Cainey, A. L. Dick, Chloride and bromide loss from sea-salt particles in southern ocean air. *J. Atmos. Chem.* **33**, 299–319 (1999).
28. R. Gabriel, R. von Glasow, R. Sander, M. O. Andreae, P. J. Crutzen, Bromide content of sea-salt aerosol particles collected over the Indian Ocean during INDOEX 1999. *J. Geophys. Res. Atmos.* **107**, INX2 31-31–INX32 31-39 (2002).
29. R. M. Chambers, A. C. Heard, R. P. Wayne, Inorganic gas-phase reactions of the nitrate radical: Iodine + nitrate radical and iodine atom + nitrate radical. *J. Phys. Chem.* **96**, 3321–3331 (1992).
30. N. S. Holmes, J. W. Adams, J. N. Crowley, Uptake and reaction of HOI and $IONO_2$ on frozen and dry NaCl/NaBr surfaces and H_2SO_4. *Phys. Chem. Chem. Phys.* **3**, 1679–1687 (2001).
31. A. S. Mahajan *et al*., Reactive iodine species in a semi-polluted environment. *Geophys. Res. Lett.* **36**, L16803 (2009).
32. A. Saiz-Lopez *et al*., Nighttime atmospheric chemistry of iodine. *Atmos. Chem. Phys.* **16**, 15593–15604 (2016).
33. B. J. Allan, J. M. C. Plane, H. Coe, J. Shillito, Observations of NO3 concentration profiles in the troposphere. *J. Geophys. Res. Atmos.* **107**, ACH 11-11–ACH 11-14 (2002).
34. H. Coe *et al*., Chemical and physical characteristics of aerosol particles at a remote coastal location, Mace Head, Ireland, during NAMBLEX. *Atmos. Chem. Phys.* **6**, 3289–3301 (2006).
35. M. Wachsmuth, H. W. Gäggeler, R. von Glasow, M. Ammann, Accommodation coefficient of HOBr on deliquescent sodium bromide aerosol particles. *Atmos. Chem. Phys.* **2**, 121–131 (2002).
36. M. Ammann *et al*., Evaluated kinetic and photochemical data for atmospheric chemistry: Volume VI – heterogeneous reactions with liquid substrates. *Atmos. Chem. Phys.* **13**, 8045–8228 (2013).
37. M. J. Rossi, Heterogeneous reactions on salts. *Chem. Rev.* **103**, 4823–4882 (2003).
38. I. J. George, J. P. Abbatt, Heterogeneous oxidation of atmospheric aerosol particles by gas-phase radicals. *Nat. Chem.* **2**, 713–722 (2010).
39. S.-M. Fan, D. J. Jacob, Surface ozone depletion in Arctic spring sustained by bromine reactions on aerosols. *Nature* **359**, 522–524 (1992).
40. W. C. Keene *et al*., Aerosol pH in the marine boundary layer: A review and model evaluation. *J. Aerosol Sci.* **29**, 339–356 (1998).
41. J. Ovadnevaite *et al*., Submicron NE Atlantic marine aerosol chemical composition and abundance: Seasonal trends and air mass categorization. *J. Geophys. Res. Atmos.* **119**, 11,850–11,863 (2014).
42. C. Ordóñez *et al*., Bromine and iodine chemistry in a global chemistry-climate model: Description and evaluation of very short-lived oceanic sources. *Atmos. Chem. Phys.* **12**, 1423–1447 (2012).
43. T. Sherwen *et al*., Iodine's impact on tropospheric oxidants: A global model study in GEOS-Chem. *Atmos. Chem. Phys.* **16**, 1161–1186 (2016).
44. B. Alicke, K. Hebestreit, J. Stutz, U. Platt, Iodine oxide in the marine boundary layer. *Nature* **397**, 572–573 (1999).
45. L. K. Whalley *et al*., Detection of iodine monoxide radicals in the marine boundary layer using laser induced fluorescence spectroscopy. *J. Atmos. Chem.* **58**, 19–39 (2007).
46. M. J. Lawler, A. S. Mahajan, A. Saiz-Lopez, E. S. Saltzman, Observations of I_2 at a remote marine site. *Atmos. Chem. Phys.* **14**, 2669–2678 (2014).
47. A. S. Mahajan *et al*., Observations of iodine oxide in the Indian Ocean marine boundary layer: A transect from the tropics to the high latitudes. *Atmos. Environ. X* **1**, 100016 (2019).
48. A. Saiz-Lopez *et al*., Estimating the climate significance of halogen-driven ozone loss in the tropical marine troposphere. *Atmos. Chem. Phys.* **12**, 3939–3949 (2012).

49. C. Prados-Roman *et al*., A negative feedback between anthropogenic ozone pollution and enhanced ocean emissions of iodine. *Atmos. Chem. Phys.* **15**, 2215–2224 (2015).
50. A. Saiz-Lopez *et al*., Iodine chemistry in the troposphere and its effect on ozone. *Atmos. Chem. Phys.* **14**, 13119–13143 (2014).
51. X.-C. He *et al*., Determination of the collision rate coefficient between charged iodic acid clusters and iodic acid using the appearance time method. *Aerosol Sci. Technol.*, 10.1080/02786826.2020.1839013 (2020).
52. J. C. Gómez Martín *et al*., A gas-to-particle conversion mechanism helps to explain atmospheric particle formation through clustering of iodine oxides. *Nat. Commun.* **11**, 4521 (2020).
53. G. McFiggans *et al*., Iodine-mediated coastal particle formation: An overview of the reactive halogens in the marine boundary layer (RHaMBLe) Roscoff coastal study. *Atmos. Chem. Phys.* **10**, 2975–2999 (2010).
54. H. Yu *et al*., Iodine speciation and size distribution in ambient aerosols at a coastal new particle formation hotspot in China. *Atmos. Chem. Phys.* **19**, 4025–4039 (2019).
55. G. McFiggans, R. A. Cox, J. C. Mössinger, B. J. Allan, J. M. C. Plane, Active chlorine release from marine aerosols: Roles for reactive iodine and nitrogen species. *J. Geophys. Res. Atmos.* **107**, ACH 10-11–ACH 10-13 (2002).
56. S. M. MacDonald *et al*., A laboratory characterisation of inorganic iodine emissions from the sea surface: Dependence on oceanic variables and parameterisation for global modelling. *Atmos. Chem. Phys.* **14**, 5841–5852 (2014).
57. C. Prados-Roman *et al*., Iodine oxide in the global marine boundary layer. *Atmos. Chem. Phys.* **15**, 583–593 (2015).
58. A. S. Mahajan *et al*., Understanding iodine chemistry over the northern and equatorial Indian Ocean. *J. Geophys. Res. Atmos.* **124**, 8104–8118 (2019).
59. A. Saiz-Lopez *et al*., On the vertical distribution of boundary layer halogens over coastal Antarctica: Implications for O_3, HO_x, NO_x and the Hg lifetime. *Atmos. Chem. Phys.* **8**, 887–900 (2008).